

SPARSE: Scattering Poles and Amplitudes from Radial Schrödinger Equations

Roberto Bruschini*

Department of Physics, The Ohio State University, Columbus, Ohio 43210, USA

Abstract

We introduce an algorithm for the solution of a three-dimensional, two-body Schrödinger equation for scattering states. The equation is first reduced to a system of coupled radial Schrödinger equations. The system of differential equations is approximated as an ordinary linear nonhomogeneous system using the finite difference method. Dirichlet boundary conditions are imposed at the origin and at an arbitrary large radius. The physical K -matrix for real energies is calculated from the numerical solutions of this system by comparison to the analytical real solutions for large distances. Scattering amplitudes are calculated from the physical K -matrix. Scattering poles are obtained by extrapolating the K -matrix to complex energies.

PROGRAM SUMMARY

Program Title: SPARSE

CPC Library link to program files: (to be added by Technical Editor)

Developer's repository link: github.com/Robrusch/SPARSE

Licensing provisions: MIT

Programming language: Python

Nature of problem: Calculation of two-body scattering poles and amplitudes from a radial multichannel Schrödinger equation.

Solution method: We approximate the second derivative using the finite difference method. We impose Dirichelet boundary conditions and reduce the differential equation to a nonhomogeneous linear system. We obtain the K -matrix from integrals of the wavefunctions times a sine or cosine function calculated using the

*Corresponding author.

Email address: bruschini.1@osu.edu (Roberto Bruschini)

trapezoidal rule. We obtain the scattering amplitudes from the K -matrix for real energies. We obtain the scattering poles by extrapolating the K -matrix to complex energies through a rational approximation.

1. Introduction

The Schrödinger equation applies to scattering states just as well as to bound states. In fact, the Schrödinger equation provides the foundation of many approximate analytical methods to calculate scattering resonances using nonrelativistic quantum mechanics. But the advantages of calculating scattering poles and amplitudes directly from the Schrödinger equation are often overlooked.

The most obvious benefit of calculating scattering states directly from the Schrödinger equation is that it does not require any additional assumption, approximation, or parametrization that may undermine the validity of the results. The scattering amplitudes are completely determined by the Schrödinger equation, and thus they are just as good as the underlying potential. That is most advantageous for those cases where resonant line shapes overlap with one another or with the energy thresholds where scattering channels open up. There is no need of a special treatment for esoteric structures like dips and cusps in the scattering amplitudes, since they are automatically included in the Schrödinger equation.

A multichannel scattering Schrödinger equation can be used to describe the quantum mechanical scattering of particles in systems where different final states are possible after the collision. One notable example is nucleon-nucleon scattering, where the state of the colliding particles can change at relatively low scattering momentum ($NN \rightarrow NN, N\Delta, NN', \Delta\Delta, \dots$).

In this paper, we introduce a simple yet effective algorithm for calculating scattering poles and amplitudes directly from a multichannel Schrödinger equation. Our method is to solve the Schrödinger equation using a simple finite-difference method (see Chapter 3 of Reference [1]). Other common methods include propagation algorithms [2, 3] or basis expansions [4, 5] (see Reference [1] for a review).

The rest of the paper is structured as follows. In Section 2, we derive the multichannel radial Schrödinger equation describing an elastic or inelastic 2-body scattering process. In Section 3, we reduce the radial Schrödinger equation down to a nonhomogeneous linear system. In Section 4, we calculate

the reactance matrix K for the scattering process by comparing the numerical solutions of the Schrödinger equation to the analytic ones for scattering states with real boundary conditions. In Section 5, we review the calculation of scattering amplitudes from the K -matrix and we calculate scattering resonances by extrapolating to complex energies using a rational approximation. In Section 6, we showcase the SPARSE algorithm using a relatively simple example. Finally, we summarize these results in Section 7.

2. Radial Schrödinger equation

A two-body elastic or inelastic scattering process can be described by a multichannel Schrödinger equation whose most general form is

$$\left[\frac{p_1^2}{2m_1} + \frac{p_2^2}{2m_2} + V(\mathbf{r}_1 - \mathbf{r}_2) - E \right] \psi(\mathbf{r}_1, \mathbf{r}_2) = 0, \quad (1)$$

where \mathbf{r}_1 , \mathbf{r}_2 are the particles' coordinates, $\mathbf{p}_1 = -i\nabla_{\mathbf{r}_1}$, $\mathbf{p}_2 = -i\nabla_{\mathbf{r}_2}$ are their conjugate momenta, m_1 and m_2 are diagonal mass matrices, $V(\mathbf{r}_1 - \mathbf{r}_2)$ is a spin-dependent potential matrix, E is the total energy, and $\psi(\mathbf{r}_1, \mathbf{r}_2)$ is a multichannel wavefunction with spin. Note that we use natural units, $\hbar = c = 1$.

We wish to reduce Equation (1) down to a differential equation in a single vector variable. Let us introduce the relative position

$$\mathbf{r} = \mathbf{r}_1 - \mathbf{r}_2 \quad (2)$$

and the center-of-average-mass position

$$\mathbf{R} = \frac{\overline{m}_1 \mathbf{r}_1 + \overline{m}_2 \mathbf{r}_2}{\overline{m}_1 + \overline{m}_2}, \quad (3)$$

where \overline{m}_1 and \overline{m}_2 are the average of the masses in the diagonal matrices m_1 and m_2 . We also introduce the relative momentum

$$\mathbf{p} = \frac{\overline{m}_2 \mathbf{p}_1 - \overline{m}_1 \mathbf{p}_2}{\overline{m}_1 + \overline{m}_2} \quad (4)$$

and the total momentum

$$\mathbf{P} = \mathbf{p}_1 + \mathbf{p}_2, \quad (5)$$

which are the momenta conjugate to \mathbf{r} and \mathbf{R} , $\mathbf{p} = -i\nabla_{\mathbf{r}}$ and $\mathbf{P} = -i\nabla_{\mathbf{R}}$. Expressing \mathbf{r}_1 , \mathbf{r}_2 , \mathbf{p}_1 , and \mathbf{p}_2 inside Equation (1) in terms of \mathbf{r} , \mathbf{R} , \mathbf{p} , and \mathbf{P} using Equations (2)-(5), we obtain

$$\left[\frac{p^2}{2\mu} + \left(\frac{\bar{m}_1}{m_1} - \frac{\bar{m}_2}{m_2} \right) \frac{\mathbf{p} \cdot \mathbf{P}}{\bar{m}_1 + \bar{m}_2} + \left(\frac{\bar{m}_1^2}{m_1} + \frac{\bar{m}_2^2}{m_2} \right) \frac{P^2}{2(\bar{m}_1 + \bar{m}_2)^2} + V(\mathbf{r}) - E \right] \psi(\mathbf{r}, \mathbf{R}) = 0, \quad (6)$$

where

$$\mu = \frac{m_1 m_2}{m_1 + m_2} \quad (7)$$

is a diagonal reduced-mass matrix. The Schrödinger equation is separable if the matrix multiplying $\mathbf{p} \cdot \mathbf{P}$ is zero, which requires

$$\frac{\bar{m}_1}{m_1} = \frac{\bar{m}_2}{m_2}. \quad (8)$$

In this case, Equation (6) becomes

$$\left[\frac{p^2}{2\mu} + \frac{P^2}{2(m_1 + m_2)} + V(\mathbf{r}) - E \right] \psi(\mathbf{r}, \mathbf{R}) = 0. \quad (9)$$

Then, separating \mathbf{R} and its conjugate momentum \mathbf{P} from Equation (9) produces a differential equation in the single vector variable \mathbf{r} ,

$$\left[\frac{p^2}{2\mu} + V(\mathbf{r}) - E \right] \psi(\mathbf{r}) = 0, \quad (10)$$

where E now represents the energy in the center-of-momentum frame where $\mathbf{P} = 0$. Note that the separability condition in Equation (8) is satisfied exactly if and only if the two mass matrices are linearly dependent, $m_1 \propto m_2$. If m_1 and m_2 are linearly independent, Equation (8) cannot be satisfied exactly but Equation (6) may be approximately separable if

$$\left\| \frac{\bar{m}_1}{m_1} - \frac{\bar{m}_2}{m_2} \right\| \ll 1, \quad (11)$$

where the double vertical lines denote the matrix norm.

Equation (10) is a differential equation for a multichannel vector wavefunction $\psi(\mathbf{r})$ of the relative position vector \mathbf{r} . We wish to further reduce it

to an equation for a multichannel radial wavefunction $\psi(r)$ of the distance $r = |\mathbf{r}|$. Let us label the channels of the Schrödinger equation by a . The Schrödinger equation in the channel a reads

$$\sum_b \left[\delta_{ab} \frac{p^2}{2\mu_a} + V_{ab}(\mathbf{r}) - \delta_{ab} E \right] \psi_b(\mathbf{r}) = 0, \quad (12)$$

where $\psi_b(\mathbf{r})$ is a vector wavefunction component and $V_{ab}(\mathbf{r})$ are potential matrix elements. Let α_a and β_a be the two particles in the channel a with spins J_{α_a} and J_{β_a} , respectively. We can expand the vector wavefunction $\psi_a(\mathbf{r})$ as

$$\psi_a(\mathbf{r}) = \sum_{s,l} \sum_{\sigma,m} \psi_{a,s,l}^{\sigma,m}(r) Y_l^m(\theta, \phi) \xi_s^\sigma, \quad (13)$$

where $\psi_{a,l,s}^{\sigma,m}(r)$ are radial wavefunctions, $Y_l^m(\theta, \phi)$ are spherical harmonics, and ξ_s^σ are irreducible representations from the decomposition of the direct product of the spin states $\chi_{J_{\alpha_a}}^{M_{\alpha_a}}$ and $\chi_{J_{\beta_a}}^{M_{\beta_a}}$ of the two particles α_a and β_a ,

$$\xi_s^\sigma = \sum_{M_{\alpha_a}, M_{\beta_a}} \langle J_{\alpha_a} J_{\beta_a} M_{\alpha_a} M_{\beta_a} | J_{\alpha_a} J_{\beta_a} s\sigma \rangle \chi_{J_{\alpha_a}}^{M_{\alpha_a}} \chi_{J_{\beta_a}}^{M_{\beta_a}}, \quad (14)$$

where the term with angle brackets is a Clebsch-Gordan coefficient. The sum over the spin quantum number s ranges from $|J_{\alpha_a} - J_{\beta_a}|$ to $J_{\alpha_a} + J_{\beta_a}$, and for each s the sum over the third component σ ranges from $-s$ to $+s$. The sum over the orbital-angular-momentum quantum number l ranges from 0 to infinity, and for each l the sum over the third component m ranges from $-l$ to $+l$. The radial wavefunctions in Equation (13) are labeled by quantum numbers σ and m for the third components of the spin and orbital angular momentum. It is more convenient to rewrite Equation (13) as an expansion in radial wavefunctions labeled by quantum numbers J and M for the total angular momentum,

$$\psi_a(\mathbf{r}) = \sum_{J,M} \sum_{s,l} \psi_{a,s,l}^{JM}(r) \sum_{\sigma,m} \langle sl\sigma m | slJM \rangle Y_l^m(\theta, \phi) \xi_s^\sigma. \quad (15)$$

The sum over J ranges from either 0 or $\frac{1}{2}$ to infinity, and for each J the sum over the third component M ranges from $-J$ to $+J$.

We derive the Schrödinger equation for the radial wavefunctions through the following steps:

- (i) Substitute Equation (15) into (12).
- (ii) Multiply on the left by $\sum_{\sigma', m'} \langle s' l' \sigma' m' | s' l' J' M' \rangle Y_l^{m'*}(\theta, \phi) \xi_{s'}^{\sigma' \dagger}$.
- (iii) Integrate over the solid angle Ω .
- (iv) Impose conservation of angular momentum.

Once the above procedure has been applied to each channel a , the Schrödinger equation for the multichannel radial wavefunction $\psi^{JM}(r)$ with total angular momentum J and third component M can be written concisely as

$$\left[\frac{1}{2\mu} \left(-\frac{d^2}{dr^2} - \frac{2}{r} \frac{d}{dr} + \frac{L(L+1)}{r^2} \right) + V^J(r) - E \right] \psi^{JM}(r) = 0, \quad (16)$$

where L is a diagonal orbital-angular-momentum matrix, $V^J(r)$ is a radial potential matrix, and each channel a of the three-dimensional Schrödinger equation has been expanded into spin-orbital channels (a, l, s) . Note that s and l are constrained by the triangle relations $|J_{\alpha_a} - J_{\beta_a}| \leq s \leq J_{\alpha_a} + J_{\beta_a}$ and $|J - s| \leq l \leq J + s$, so that each channel a expands into a finite number of spin-orbital channels (a, l, s) for each J . To simplify the notation, we relabel the spin-orbital channels of the radial wavefunction by a single integer i . Then the radial potential matrix element for the spin-orbital channels i and j is given by

$$V_{ij}^J(r) = \sum_{\sigma_i, m_i} \sum_{\sigma_j, m_j} \langle s_i l_i \sigma_i m_i | s_i l_i JM \rangle \langle s_j l_j \sigma_j m_j | s_j l_j JM \rangle \times \int d\Omega Y_l^{m_i*}(\theta, \phi) Y_l^{m_j}(\theta, \phi) \xi_{s_i}^{\sigma_i \dagger} V_{ab}(\mathbf{r}) \xi_{s_j}^{\sigma_j}, \quad (17)$$

where $(a, s_i, l_i) \mapsto i$, $(b, s_j, l_j) \mapsto j$, and the spin vectors $\xi_{s_i}^{\sigma_i \dagger}$ and $\xi_{s_j}^{\sigma_j}$ can be expanded in terms of the spin vectors of the individual particles $\chi_{J_{\alpha_i}}^{M_{\alpha_i}}, \chi_{J_{\beta_i}}^{M_{\beta_i}}$ and $\chi_{J_{\alpha_j}}^{M_{\alpha_j}}, \chi_{J_{\beta_j}}^{M_{\beta_j}}$ using Equation (14). Note that the right side of Equation (17) does not actually depend on M by virtue of the Wigner-Eckart theorem.

There is a somewhat common misunderstanding that the reduction of a three-dimensional Schrödinger equation to a radial form can be performed only for a spherically-symmetric potential that does not depend on the angles θ and ϕ . However, in our derivation of Equations (16) and (17) we have made no assumption on the potential $V(\mathbf{r})$ other than it conserves angular momentum. In the trivial case where the potential is independent of spin, then conservation of angular momentum does indeed require that it is also

spherically symmetric. If the potential does depend on spin, then it can also depend on the angles θ and ϕ but the reduction to Equation (16) would still apply. A brute-force method to determine if any given potential $V(\mathbf{r})$ conserves angular momentum is to evaluate the right side of Equation (17) with J and M in the first Clebsch-Gordan coefficient substituted by J' and M' . The potential $V(\mathbf{r})$ conserves angular momentum if and only if the result is zero unless $J' = J$ and $M' = M$ and it is independent of M .

Equation (16) describes a scattering process taking place in a partial wave labeled by quantum numbers J and M . Because of conservation of angular momentum, each partial wave is decoupled from the others. SPARSE solves the scattering problem only for one individual partial wave, leaving the task of summing partial waves to the user. Hence, from now on we will drop all superscripts for the conserved quantum numbers J and M .

Finally, we can simplify the derivatives inside Equation (16) as follows. Let us observe that

$$\left(\frac{d^2}{dr^2} + \frac{2}{r} \frac{d}{dr} \right) \psi(r) = \frac{1}{r} \frac{d^2}{dr^2} u(r), \quad (18)$$

where we have introduced the reduced radial wavefunction

$$u(r) = r\psi(r). \quad (19)$$

Substituting Equation (18) into (16) and multiplying both sides by r yields

$$\left[-\frac{1}{2\mu} \frac{d^2}{dr^2} + \frac{L(L+1)}{2\mu r^2} + V(r) - E \right] u(r) = 0. \quad (20)$$

Equation (20) is the form of the Schrödinger equation solved by the SPARSE algorithm. It has N spin-orbital channels labeled by an integer $i = 1, 2, \dots, N$. The channel i has spin s_i and orbital angular momentum l_i . The reduced-mass matrix elements are $\mu_{ij} = \delta_{ij}\mu_i$. The orbital-angular-momentum matrix elements are $L_{ij} = \delta_{ij}l_i$. The radial potential matrix elements $V_{ij}(r)$ can be determined by evaluating Equation (17) for a given potential $V(\mathbf{r})$.

3. Numerical solution

To solve Equation (20) numerically, we truncate and discretize the coordinate space from the real positive numbers to a finite grid of equally-spaced points $\{r_n\}_{n=0}^{M+1}$, where

$$r_n = nd \quad (21)$$

with d a small discretization step. Our discretized coordinate space begins at the origin $r_0 = 0$, has M points in its interior that we refer to as nodes, and ends at a finite but otherwise arbitrarily large radius $r_{M+1} = R$. We define the numerical reduced radial wavefunction in channel i as $u_i(r_n)$. Similarly, we define the numerical potential matrix element between the channels i and j as $V_{ij}(r_n)$. We then use the Calculus of Finite Differences to approximate the second derivative of the wavefunction as

$$\frac{d^2}{dr^2}u(r_n) = \frac{u(r_{n-1}) - 2u(r_n) + u(r_{n+1})}{d^2} + \mathcal{O}(d^4). \quad (22)$$

For small enough discretization steps d , the $\mathcal{O}(d^4)$ corrections can be neglected.

To close the system of equations, we fix the values of the reduced radial wavefunction at the boundaries, $u_i(0)$ and $u_i(R)$. This is referred to as imposing Dirichlet boundary conditions. We can choose the appropriate boundary conditions using the known analytical behavior of the solutions to Equation (20) for $r \rightarrow 0$ and $r \rightarrow \infty$. Since a physical solution $u_i(r)$ goes to zero as r^{l_i+1} for $r \rightarrow 0$, we impose

$$u_i(0) = 0. \quad (23)$$

The other boundary condition, $u_i(R)$, is more complicated. We define the threshold matrix as $T = \lim_{r \rightarrow \infty} V(r)$. For scattering problems,

$$\lim_{r \rightarrow \infty} V_{ij}(r) = \delta_{ij} T_i \quad (24)$$

so the threshold matrix T is diagonal. Each threshold value T_i is either a definite number or positive infinity. If T_i is a finite number, then $|V_{ii}(r) - T_i|$ must approach zero faster than $1/r$ and $V_{ij}^2(r)/|V_{jj}(r) - T_i|$ must approach zero faster than $1/r$ for every $j \neq i$. The boundary condition $u_i(R)$ depends on whether the corresponding threshold T_i is larger or smaller than the energy E in the Schrödinger equation. If $T_i > E$, then a physical solution goes to zero for $r \rightarrow \infty$ and we impose $u_i(R) = 0$. If otherwise $T_i \leq E$, a physical solution keeps oscillating indefinitely for $r \rightarrow \infty$. It is however a specific, finite number at the maximum distance R in our truncated coordinate space. So, we impose $u_i(R) = b_i$, where b_i is a real constant. We can conveniently impose the boundary condition for both $E \geq T_i$ and $E < T_i$ at once in the form

$$u_i(R) = \theta(E - T_i) b_i, \quad (25)$$

where

$$\theta(x) = \begin{cases} 1 & \text{if } x \geq 0, \\ 0 & \text{if } x < 0, \end{cases} \quad (26)$$

is the Heaviside step function.

Using Equations (22), (23), and (25), we derive from Equation (20) the numerical Schrödinger equation

$$\sum_{j,m} [H_{ij,nm} - \delta_{ij}\delta_{nm}E] u_j(r_m) = \delta_{nM}\theta(E - T_i) \frac{b_i}{2\mu_i d^2}, \quad (27)$$

where $H_{ij,nm}$ are the numerical Hamiltonian matrix elements

$$H_{ij,nm} = -\delta_{ij} \frac{\delta_{(n-1)m} - 2\delta_{nm} + \delta_{(n+1)m}}{2\mu_i d^2} + \delta_{ij}\delta_{nm} \frac{l_i(l_i + 1)}{2\mu_i r_n^2} + \delta_{nm}V_{ij}(r_n) \quad (28)$$

with $i, j = 1, \dots, N$ denoting channels and $n, m = 1, \dots, M$ denoting nodes. The Hamiltonian is a matrix with $N^2 M^2$ elements, but only a small fraction of those are different from zero. The ratio of nonzero elements over the total scales like $1/M$, with M being a very large number for a large maximum distance R and a small discretization step d . The Hamiltonian in Equation (28) is therefore a sparse matrix.

To input the Schrödinger equation into SPARSE, the user has to provide the following information:

- The orbital angular momentum l_i , reduced mass μ_i , and threshold T_i for each channel i .
- The positions of the nodes r_n and the numerical potential matrix elements $V_{ij}(r_n)$.

SPARSE reads this information from two comma-separated-values (CSV) files named `channels.csv` and `potential.csv`, which must be placed within the working directory.

The file `channels.csv` must have one line for the header followed by N lines for the values. Each line must contain at least three entries. The header must contain at least the following strings: `l`, `mu`, and `threshold`. The following N lines must contain at least the corresponding values for the channels $i = 1, \dots, N$. An entry under `l` is an integer indicating l_i . An entry under `mu` is a decimal number indicating μ_i . An entry under `threshold` is a

decimal number indicating T_i or `inf` if $T_i = \infty$. The ordering of the columns is irrelevant, but it must obviously be consistent between rows. Below is the typical structure of a minimal `channels.csv` file.

```
1,mu,threshold
11,mu1,T1
12,mu2,T2
...
1N,muN,TN
```

For the user's convenience, additional information about the channels may be specified by adding more columns to the file `channels.csv`. For instance, the user may want to include a column named `s` indicating the spin s_i for each channel i , or a column named `channel` providing a label for each channel that is more informative than just the integer i . Such additional columns will be read by SPARSE but will not play any role in the calculation.

The file `potential.csv` must have no header and M lines for the values. Each line must contain exactly $N^2 + 1$ entries. The first entry is the node position r_n . The following N^2 entries are the numerical values of the flattened potential matrix, $V_{ij}(r_n)$. SPARSE assumes that the potential matrix is flattened in row-major (C-style) order.¹ Below is the typical structure of the `potential.csv` file.

```
r1,V11(r1),V12(r1),...,VNN(r1)
r2,V11(r1),V12(r2),...,VNN(r2)
...
rM,V11(rM),V12(rM),...,VNN(rM)
```

SPARSE reads the values from the two CSV files and writes them inside two pandas `DataFrame` objects using the function `read_csv` from pandas [6]. From them, SPARSE calculates the Hamiltonian matrix elements $H_{ij,nm}$ from Equation (28) and writes them into a 2-dimensional NumPy `array` object [7] with elements $H_{\alpha\beta}$. This reshaping amounts to applying an invertible map $(i, n) \mapsto \alpha$ from pairs of indices $i = 1, \dots, N$ and $n = 1, \dots, M$ to a single index $\alpha = 1, \dots, NM$. SPARSE reads the matrix elements from Equation (28) and writes them in the NumPy `array` following a C-style

¹This fact is irrelevant if the potential is a symmetric matrix.

index order, which corresponds to setting

$$\alpha = i + N(n - 1). \quad (29)$$

This choice of index order has the advantage that all the nonzero $H_{\alpha\beta}$ end up as close as possible to the main diagonal $\alpha = \beta$. From Equation (28), we see that the only nonzero $H_{ij,nm}$ are those with $|i - j| \leq N - 1$ and $n = m$ or $|n - m| \leq 2$ and $i = j$. Then it follows from Equation (29) that the only nonzero $H_{\alpha\beta}$ are those with

$$|\alpha - \beta| \leq |i - j| + N|n - m| \leq 2N. \quad (30)$$

Therefore the $H_{\alpha\beta}$ form a banded matrix with N nonzero upper diagonals and N nonzero lower diagonals, $\alpha = \beta - \gamma$ and $\alpha = \beta + \gamma$ with $\gamma = 1, \dots, N$.

SPARSE writes the Hamiltonian in the matrix diagonal ordered form, which is a 2-dimensional array consisting of only the $2N+1$ nonzero diagonals stacked from top to bottom. The upper and lower diagonals are padded so that they all have the same number of elements NM as the main diagonal. The matrix diagonal ordered form has only $(2N + 1) \times (NM)$ elements, and therefore it occupies significantly less memory than the full $(NM) \times (NM)$ matrix with its many zeroes. Consider for example a system with $N = 4$ channels and $M = 10^6$ nodes using 64-bit floating-point numbers. The matrix diagonal ordered form would take 288 megabytes of memory, opposed to a staggering 128 terabytes for the full matrix! Without the matrix diagonal ordered form, it would be all but impossible to accurately solve the Schrödinger equation using the finite-difference method.

So, we redefine the indices of Equation (27) as $(i, n) \mapsto \alpha$ and $(j, m) \mapsto \beta$ using Equation (29) and we obtain an ordinary nonhomogeneous linear system,

$$\sum_{\beta} (H_{\alpha\beta} - \delta_{\alpha\beta}E)u_{\beta} = B_{\alpha}(E), \quad (31)$$

where the constant vector is

$$B_{\alpha}(E) = \delta_{nM}\theta(E - T_i)\frac{b_i}{2\mu_i d^2}. \quad (32)$$

Note that if $E < T_i$ for all i , which corresponds to a bound state, then $B_{\alpha}(E) = 0$ for all α and Equation (31) becomes an eigenvalue problem for the Hamiltonian matrix. Even though SPARSE is primarily designed for

scattering problems, it also contains a handy bound-state calculator which solves Equation (31) with $B_\alpha(E) = 0$ using the function `eigsh` from the sparse linear algebra module of SciPy [8].

Finally, a note about measuring units. SPARSE uses natural units, in which $\hbar = c = 1$ and therefore [Time] = [Length], [Mass] = [Energy], and [Length] = [Energy] $^{-1}$. There is only one independent dimension, typically chosen between [Length] in units of fm (femtometers) and [Energy] in units of eV (electron Volts). The SPARSE algorithm is agnostic to the user's choices of dimension and unit, as long as it is consistent with the prescription $\hbar = c = 1$. The conversion between length-based and energy-based units is easily achieved by means of the formula $\hbar c = 1 = 197.327$ MeV fm.

4. Calculating the K -matrix

From now on we shall assume, without loss of generality, that the channels i are ordered in increasing threshold value, $T_i \geq T_j$ for any $i \geq j$.² For a given energy E , the possible values of the constant in Equation (32) constitute a vector space of dimension O , where O is the number of open channels i whose threshold is less than E , $T_i \leq E$ for $i = 1, \dots, O$. We can easily construct a basis for this vector space by substituting b_i inside Equation (32) with

$$b_{ij} = \delta_{ij}, \quad (33)$$

where the first index $i = 1, \dots, N$ labels the channels and the second index $j = 1, \dots, O$ labels the vectors in the basis. We treat the b_{ij} from Equation (33) as the elements of a $N \times O$ matrix b , and the result of plugging Equation (33) into (32) as the elements of a $(NM) \times O$ matrix B , dropping its dependence on E . We also define the $(NM) \times (NM)$ matrix

$$A = H - EI. \quad (34)$$

with I the identity matrix. A is a banded matrix which SPARSE calculates by shifting the main diagonal of the Hamiltonian by $-E$ in the matrix diagonal ordered form. With these definitions, we rewrite Equation (31) as a matrix equation

$$Au = B, \quad (35)$$

²This assumption is made in the paper for the sake of simplifying the notation. The SPARSE algorithm does not require the input channels to be sorted in any particular way.

where u is a $(NM) \times O$ matrix whose columns are the linearly independent solutions to Equation (31) with the same energy E .

For any energy E , SPARSE constructs the matrices A and B using Equations (32)-(34) and solves Equation (35) for the matrix u using the function `solve_banded` from the linear algebra module of SciPy [8]. Then, SPARSE obtains the numerical wavefunctions from the matrix elements of u using Equation (29), $u_{\alpha j} \rightarrow u_{ij}(r_n)$. Next, we use these numerical solutions to calculate the reactance matrix K for the scattering process. We will disregard from now on wavefunction components for confining channels with $T_i = \infty$, which are irrelevant to the scattering states at large r .

First, we define the numerical range of the potential r_V as the maximum value of r for which the potential matrix is significantly different from the threshold matrix (excluding diagonal elements for confining channels),

$$r_V = \max\{r \mid \|V(r) - T\| > \epsilon\}, \quad (36)$$

where ϵ is a fixed small number.

Next, we review the analytic asymptotic solution at large r . For $r > r_V$, Equation (20) reduces to a set of decoupled Schrödinger equations for free particles,

$$\left[-\frac{1}{2\mu_i} \frac{d^2}{dr^2} + \frac{l_i(l_i + 1)}{2\mu r^2} + T_i - E \right] u_i(r) = 0 \quad (37)$$

for every channel i with a finite threshold T_i . Solutions to Equation (37) for closed channels $i = O + 1, \dots, N$ with $T_i > E$ must approach zero at large distances and are irrelevant to the scattering states. For the open channels $i = 1, \dots, O$ with $T_i \leq E$, Equation (37) has two linearly independent solutions. Using real boundary conditions and wavefunction normalization by energy (see Reference [9] for alternative conventions), the two solutions are

$$\sqrt{\frac{2\mu_i}{\pi p_i}} S_{l_i}(p_i r) \quad \text{and} \quad \sqrt{\frac{2\mu_i}{\pi p_i}} C_{l_i}(p_i r), \quad (38)$$

where p_i is the scattering momentum in the channel i ,

$$p_i = \sqrt{2\mu_i(E - T_i)}, \quad (39)$$

and $S_l(x)$ and $C_l(x)$ are the Riccati-Bessel functions

$$S_l(x) = x j_l(x), \quad (40)$$

$$C_l(x) = -x y_l(x), \quad (41)$$

with $j_l(x)$ and $y_l(x)$ the spherical Bessel functions of the first and second kind. The asymptotic solution of any Schrödinger equation that coincides with Equation (37) at large r can be written as a linear combination of the solutions in Equation (38). In particular, the asymptotic wavefunctions of a complete set of scattering states with energy E can be expressed as

$$u_{ij}(r) \simeq \sqrt{\frac{2\mu_i}{\pi p_i}} (S_{l_i}(p_i r) + K_{ij} C_{l_i}(p_i r)), \quad (42)$$

where the relation “ \simeq ” stands for equality at large r , the first index $i = 1, \dots, O$ labels open channels, the second index $j = 1, \dots, O$ labels linearly independent solutions with the same energy, and K_{ij} are K -matrix elements (see Section 11.1.2 of Reference [10]).

Next, we compare the numerical solutions $u_{ij}(r_n)$ to the analytic asymptotic solution in Equation (42) to extract the K -matrix elements. The numerical wavefunctions calculated from Equation (27) generally do not correspond to the asymptotic scattering states in Equation (42). Instead, the numerical wavefunctions at large r correspond to a more general linear combination of Riccati-Bessel functions,

$$u_{ij}(r) \simeq \sqrt{\frac{2\mu_i}{\pi p_i}} (X_{ij} S_{l_i}(p_i r) + Y_{ij} C_{l_i}(p_i r)), \quad (43)$$

where X_{ij} and Y_{ij} are real constants that can be regarded as the elements of two matrices X and Y . Comparing Equations (42) and (43), we see that the K -matrix can be calculated from the matrices X and Y using

$$K = YX^{-1}. \quad (44)$$

The matrices X and Y depend on the matrix constant B in Equation (35), but not the K -matrix. If instead of B we had chosen any other admissible B' , then instead of X and Y we would have obtained $X' = XW$ and $Y' = YW$ with W an invertible $O \times O$ matrix. However, the K -matrix from Equation (44) would have been the same.

Finally, let us calculate explicitly the matrices X and Y from the numerical wavefunctions $u_{ij}(r_n)$. Let us take the asymptotic solution in Equation (43) and take the further limit $x \gg l$ for the arguments of the Riccati-Bessel functions $S_l(x)$ and $C_l(x)$, which yields

$$u_{ij}(r) \simeq \sqrt{\frac{2\mu_i}{\pi p_i}} \left(X_{ij} \sin\left(p_i r - l_i \frac{\pi}{2}\right) + Y_{ij} \cos\left(p_i r - l_i \frac{\pi}{2}\right) \right). \quad (45)$$

Then consider the integrals

$$\int_{x_0}^{x_0+\pi} \sin^2(x) dx = \int_{x_0}^{x_0+\pi} \cos^2(x) dx = \frac{\pi}{2} \quad (46)$$

and

$$\int_{x_0}^{x_0+\pi} \sin(x) \cos(x) dx = 0, \quad (47)$$

where x_0 can be any real number. Using Equations (46) and (47), we obtain

$$X_{ij} = \sqrt{\frac{2p_i^3}{\pi\mu_i}} \int_a^b u_{ij}(r) \sin\left(p_i r - l_i \frac{\pi}{2}\right) dr, \quad (48)$$

$$Y_{ij} = \sqrt{\frac{2p_i^3}{\pi\mu_i}} \int_a^b u_{ij}(r) \cos\left(p_i r - l_i \frac{\pi}{2}\right) dr, \quad (49)$$

where the limits of the integrals are

$$a = R - \pi/p_i \quad \text{and} \quad b = R, \quad (50)$$

with R the maximum radius in the truncated coordinate space. Evaluating Equations (48) and (49) using the numerical wavefunctions $u_{ij}(r_n)$ and the trapezoidal rule provides a way of calculating X_{ij} and Y_{ij} that is both fast and numerically stable. SPARSE uses the `trapezoid` function from the integration module of SciPy [8].

5. Scattering amplitudes and resonances

We define the transition matrix T in terms of the scattering matrix S as

$$S = I + 2iT. \quad (51)$$

With this definition, a T -matrix element T_{ij} corresponds to the partial-wave scattering amplitude $f_{i \leftarrow j}$ from an initial channel j to a final channel i times the relative momentum in the final channel,

$$T_{ij} = p_i f_{i \leftarrow j}. \quad (52)$$

Scattering resonances are associated with poles of the scattering amplitude for energies in the lower half of the complex plane.

The reactance matrix K is defined as the Caley transform of the S -matrix,

$$K = i \frac{I - S}{I + S}, \quad (53)$$

which can be inverted to give

$$S = \frac{I + iK}{I - iK} \quad (54)$$

(see Section 14-e of Reference [11]). We see from Equations (53) and (54) that unitarity ($S^\dagger = S^{-1}$) and time-reversal symmetry ($S^T = S$) require that the K -matrix is real and symmetric. The K -matrix calculated using Equations (44), (48), and (49) is real by definition. It is only approximately symmetric within numerical errors. Let us call this approximately symmetric matrix \tilde{K} . SPARSE calculates the degree of asymmetry as

$$\max_{ij} \left\{ \frac{|\tilde{K}_{ij} - \tilde{K}_{ji}|}{|\tilde{K}_{ij} + \tilde{K}_{ji}|} \right\} \quad (55)$$

and warns the user if it is larger than a tolerance (1% by default). Then, SPARSE calculates the exactly symmetric K -matrix as

$$K = \frac{\tilde{K} + \tilde{K}^t}{2}. \quad (56)$$

The scattering amplitudes $f_{i \leftarrow j}$ can be calculated from the numerical K -matrix elements by inserting Equation (54) into (51), which gives

$$T = \frac{K}{I - iK}, \quad (57)$$

an using (57). The corresponding partial-wave cross-section, $\sigma_{i \leftarrow j}$, is proportional to the square modulus of the scattering amplitudes,

$$\sigma_{i \leftarrow j} = \frac{4\pi(2J+1)}{(2J_{\alpha_j}+1)(2J_{\beta_j}+1)} |f_{i \leftarrow j}|^2, \quad (58)$$

where J is the total angular momentum and J_{α_j} and J_{β_j} are the spins of the two scattering particles α_j and β_j in the initial channel j . The total unpolarized cross section can be obtained by summing over the spins s_i , s_j , the orbital angular momenta l_j , l_i , and the total angular momentum J .

From Equation (57), we see that the scattering amplitude has a pole whenever the denominator on the right side is a singular (i.e., noninvertible) matrix. We can therefore find scattering resonances from the zeros of the function

$$F(E) = \det(I - iK(E)) \quad (59)$$

for values of E in the complex plane, where we have marked the energy dependence explicitly.

SPARSE calculates the K -matrix only for real energies, therefore the zeros of $F(E)$ must be found by extrapolating from the real axis to the complex plane. One way to do this is through the use of a rational approximation, where the function $F(E)$ is approximated by the ratio of two polynomials $N(E)$ and $D(E)$,

$$F(E) \approx \frac{N(E)}{D(E)}, \quad (60)$$

which allows for the extrapolation to complex values of E . SPARSE uses the AAA algorithm for rational polynomial approximation [12] or, more precisely, its implementation as the function `AAA` in the interpolation module of SciPy [8]. The zeros and poles of $F(E)$ are then found as zeros of $N(E)$ and $D(E)$, respectively.

One known complication when dealing with rational approximations is the occurrence of near-zero residue poles or pole pairs with opposite residues that are so close as to nearly cancel each other. Since the AAA rational approximation typically has as many zeros as poles, the appearance of spurious poles of $F(E)$ would result in spurious zeros, which could be mistakenly identified as scattering resonances. To avoid the occurrence of such spurious poles, the user must first identify them and then adjust the parameters of the AAA algorithm to prevent their appearance. Luckily, it is very easy to identify spurious poles in the rational approximation of $F(E)$. In fact, the poles of $F(E)$ from Equation (59) must coincide with the poles of the K -matrix, which are located exclusively on the real energy axis. Since SPARSE can calculate the K -matrix for real energies, it is usually possible to roughly establish the number and the positions of the K -matrix poles quite reliably. Therefore, the user has only to adjust the parameters of the AAA algorithm until the poles of the rational approximation of $F(E)$ are compatible with the poles of the K -matrix. Once the poles have been identified as genuine, the zeros can be reliably identified with scattering resonances.

Table 1: Integer label i , orbital angular momentum l , threshold T , and reduced mass μ for the channels in the SPARSE showcase example. Units are arbitrary.

i	l	T	μ
1	1	0	1000
2	0	100	1000

6. Showcase

Next, we examine an application of the SPARSE algorithm to a relatively simple system with two coupled channels. The dimensions are [Energy] and [Length] = [Energy]⁻¹ with arbitrary units. The two channels are described in Table 1. The potential matrix is

$$V(r) = \begin{pmatrix} V_{11}(r) & V_{12}(r) \\ V_{21}(r) & V_{22}(r) \end{pmatrix}. \quad (61)$$

$V_{11}(r)$ is a potential well with a short-distance repulsion,

$$V_{11}(r) = \left(\frac{0.05}{r} - 100 \right) \exp(-(100r)^2) \quad (62)$$

$V_{22}(r)$ is the same potential as $V_{11}(r)$ but shifted by +100,

$$V_{22}(r) = V_{11}(r) + 100 \quad (63)$$

and $V_{12}(r) = V_{21}(r)$ is Gaussian coupling potential,

$$V_{12}(r) = 50(100r)^2 \exp(-(100r)^2). \quad (64)$$

The coordinate space of r is a grid of points in the interval $[0, 1]$ with a discretization step $d = 10^{-6}$. The potential $V_{11}(r)$ has been engineered so that it has a P -wave bound state ($l_1 = 1$) with energy somewhat below $T_1 = 0$. The potential $V_{22}(r)$ has been engineered so that in isolation it would have an S -wave bound state ($l_2 = 0$) with energy somewhat below $T_2 = 100$. The coupling potential $V_{12}(r)$ has been engineered so that the would-be bound state in the second channel appears instead as a narrow scattering resonance in the first channel. These potential matrix elements are plotted in Figure 1.

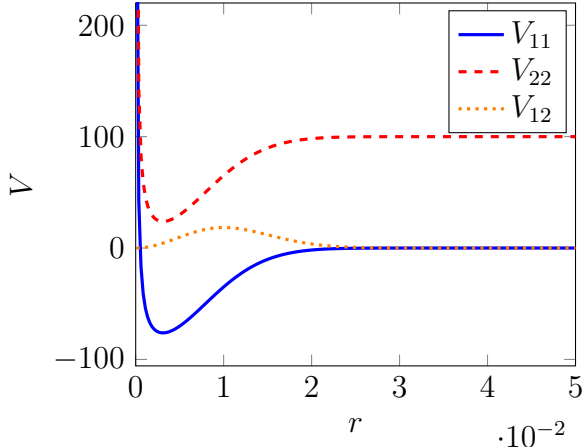


Figure 1: Potential matrix elements for the SPARSE showcase example. Axes have arbitrary units.

We use SPARSE to calculate the K -matrix for a grid of energies in the interval $[0, 80]$ with a constant spacing of 0.1. The K -matrix has only one element, since there is only one open channel in the given energy region. We plot the K -matrix as a function of the energy in Figure 2. We also calculate the square modulus of the T -matrix element and plot it in Figure 3.

The scattering amplitude looks complicated because it results from the overlap of two different line shapes. The smooth enhancement is due to the bound state in channel 1, which has an energy of -12.5. The sharp oscillation of the amplitude in between 60 and 80 is due to a resonance. That oscillation in $|T|^2$ matches a pole of the K -matrix at a similar energy. Using the AAA rational approximation to extrapolate from real energies to the complex plane, we find that there is a pole of the T -matrix located at $Z = 67.02 - 0.02i$. It corresponds to a resonance with a mass of $M = \Re(Z) = 67.02$ and a width of $\Gamma = -2\Im(Z) = 0.04$.

The SPARSE repository contains a Python script that calculates the CSV files `channels.csv` and `potential.csv` used for this example. It also contains a handy IPython notebook which reproduces the results of this section using the SPARSE Application Programming Interface.

7. Summary

SPARSE is a simple Python algorithm for the calculation of scattering amplitudes and resonances using the Schrödinger equation. It solves a sys-

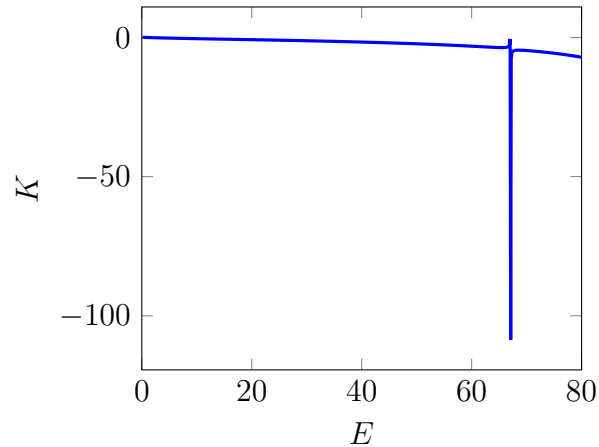


Figure 2: K -matrix for the SPARSE showcase example. The horizontal axis has arbitrary units.

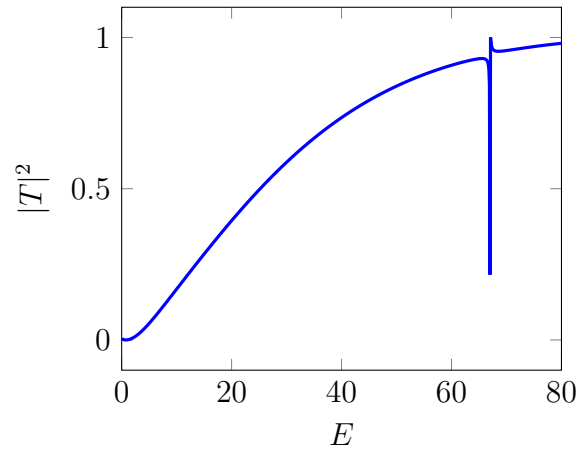


Figure 3: Square modulus of the T -matrix for the SPARSE showcase example. The horizontal axis has arbitrary units.

tem of coupled radial Schrödinger equations that represents a partial wave of a two-body scattering process. It reduces the differential equation to a non-homogeneous linear system by approximating the second derivative using the finite-difference method and imposing Dirichlet boundary conditions. It calculates the numerical wavefunctions by solving the system, then compares them to the analytical wavefunctions of scattering states to obtain the K -matrix elements. It calculates the scattering amplitudes from the K -matrix elements for real energies, then calculates resonances by extrapolating to complex energies using a rational approximation.

The only inputs required by SPARSE are the orbital angular momenta, reduced masses, and thresholds for the channels of the Schrödinger equation plus the numerical coordinate space and potential matrix. These numerical inputs are provided in the form of two CSV files named `channels.csv` and `potential.csv`. The user can calculate these numerical inputs using any computational software. The Application Programming Interface is designed so that it can be used with minimal Python literacy. The SPARSE repository also contains a Python script that creates working examples for the input CSV files. It also contains an IPython notebook which showcases the program's functionality and serves as a useful tutorial.

Acknowledgements

This work was supported in part by the U.S. Department of Energy under grant DE-SC0011726. I would like to thank F. Alasiri for beta testing the program. I would also like to thank A. Rodas for discussions during the HADRON 2025 conference.

Appendix A. Energy limits

There are limits to which scattering energies are accessible to SPARSE. Here we explain how these limits are calculated from the numerical inputs.

An overall lower energy limit is given by

$$E \geq \min_i \{T_i\}, \quad (\text{A.1})$$

since there can obviously be no scattering for energies below the lowest threshold.

An upper bound on the energy from channels with a finite threshold T_i is given by Shannon's theorem. A wavefunction is completely determined by

its values at a grid of evenly spaced points only if its wavelength is greater than twice the discretization step d ,

$$\lambda > 2d. \quad (\text{A.2})$$

Since the momentum is related to the wavelength by

$$p = \frac{2\pi}{\lambda}, \quad (\text{A.3})$$

the upper bound on the relative momentum in SPARSE is

$$p < \frac{\pi}{d}. \quad (\text{A.4})$$

Therefore, the overall limit for the energy is

$$E < \frac{\pi^2}{2\mu_i d^2} + T_i \quad (\text{A.5})$$

for all i with a finite threshold T_i . Another upper bound on the energy from confining channels with $T_i = \infty$ is given by the corresponding diagonal elements of the potential matrix. Since SPARSE assumes that the wavefunction components in confining channels is exactly zero at the maximum distance R , the energy must be much smaller than the corresponding potential at $r = R$,

$$E \ll V_{ii}(R) \quad (\text{A.6})$$

for all i with $T_i = \infty$.

The scattering energies cannot be too close to a threshold T_i , either. There is an upper bound for energies below the threshold, $E < T_i$. For a physical solution, the asymptotic wavefunction component in channel i at large r is proportional to

$$\exp(-\sqrt{2\mu_i(T_i - E)}r). \quad (\text{A.7})$$

SPARSE assumes that the wavefunction component for channels with $T_i > E$ is exactly zero at the maximum distance $r = R$, which is only a good approximation as long as the argument of the exponential satisfies

$$\sqrt{2\mu_i(T_i - E)}R \gg 1. \quad (\text{A.8})$$

Therefore we obtain an upper bound for energies below the threshold T_i ,

$$E - T_i \ll -\frac{1}{2\mu_i R^2}. \quad (\text{A.9})$$

There is also a lower bound for energies above the threshold, $E > T_i$. SPARSE uses Equations (44), (48), and (49) to calculate the K -matrix from the numerical wavefunctions of scattering states. For Equations (48) and (49) to be applicable, however, the lower limit of the integrals, $a = R - \pi/p_i$, must exceed the radius of the potential, r_Λ , which requires

$$E - T_i > \frac{\pi^2}{2\mu_i(R - r_\Lambda)^2} \quad (\text{A.10})$$

For channels with $l_i > 0$, a more stringent limit may be obtained from the condition that the argument $p_i r$ of the Riccati-Bessel functions is much greater than l_i for values in the integration domain of Equations (48) and (49). This requires

$$E - T_i \gg \frac{(l + \pi)^2}{2\mu_i R^2}. \quad (\text{A.11})$$

References

- [1] V. N. Kaliakin, *Introduction to Approximate Solution Techniques, Numerical Modeling, and Finite Element Methods*, Marcel Dekker, New York, 2002.
- [2] D. E. Manolopoulos, An improved log derivative method for inelastic scattering, *The Journal of Chemical Physics* 85 (11) (1986) 6425–6429. [doi:10.1063/1.451472](https://doi.org/10.1063/1.451472).
- [3] J. C. Butcher, A history of runge-kutta methods, *Applied numerical mathematics* 20 (3) (1996) 247–260.
- [4] S. A. Orszag, Spectral methods for problems in complex geometries, *Journal of Computational Physics* 37 (1) (1980) 70–92. [doi:10.1016/0021-9991\(80\)90005-4](https://doi.org/10.1016/0021-9991(80)90005-4).
- [5] J. Lill, G. Parker, J. Light, Discrete variable representations and sudden models in quantum scattering theory, *Chemical Physics Letters* 89 (6) (1982) 483–489. [doi:10.1016/0009-2614\(82\)83051-0](https://doi.org/10.1016/0009-2614(82)83051-0).

- [6] Wes McKinney, Data Structures for Statistical Computing in Python, in: Proceedings of the 9th Python in Science Conference, 2010, pp. 56–61. [doi:10.25080/Majora-92bf1922-00a](https://doi.org/10.25080/Majora-92bf1922-00a).
- [7] C. R. Harris, K. J. Millman, S. J. van der Walt, R. Gommers, P. Virtanen, D. Cournapeau, E. Wieser, J. Taylor, S. Berg, N. J. Smith, R. Kern, M. Picus, S. Hoyer, M. H. van Kerkwijk, M. Brett, A. Haldane, J. F. del Río, M. Wiebe, P. Peterson, P. Gérard-Marchant, K. Sheppard, T. Reddy, W. Weckesser, H. Abbasi, C. Gohlke, T. E. Oliphant, Array programming with NumPy, *Nature* 585 (7825) (2020) 357–362. [doi:10.1038/s41586-020-2649-2](https://doi.org/10.1038/s41586-020-2649-2).
- [8] P. Virtanen, R. Gommers, T. E. Oliphant, M. Haberland, T. Reddy, D. Cournapeau, E. Burovski, P. Peterson, W. Weckesser, J. Bright, S. J. van der Walt, M. Brett, J. Wilson, K. J. Millman, N. Mayorov, A. R. J. Nelson, E. Jones, R. Kern, E. Larson, C. J. Carey, İ. Polat, Y. Feng, E. W. Moore, J. VanderPlas, D. Laxalde, J. Perktold, R. Cimrman, I. Henriksen, E. A. Quintero, C. R. Harris, A. M. Archibald, A. H. Ribeiro, F. Pedregosa, P. van Mulbregt, SciPy 1.0 Contributors, SciPy 1.0: Fundamental Algorithms for Scientific Computing in Python, *Nature Methods* 17 (2020) 261–272. [doi:10.1038/s41592-019-0686-2](https://doi.org/10.1038/s41592-019-0686-2).
- [9] M. A. Morrison, A. N. Feldt, Through scattering theory with gun and camera: Coping with conventions in collision theory, *American Journal of Physics* 75 (1) (2007) 67–80. [doi:10.1119/1.2358156](https://doi.org/10.1119/1.2358156).
- [10] R. G. Newton, *Scattering Theory of Waves and Particles*, Springer Berlin, Heidelberg, 2013.
- [11] J. R. Taylor, *Scattering Theory: The Quantum Theory of Nonrelativistic Collisions*, Robert E. Krieger, Malabar, 1983.
- [12] Y. Nakatsukasa, O. Sète, L. N. Trefethen, The AAA Algorithm for Rational Approximation, *SIAM Journal on Scientific Computing* 40 (3) (2018) A1494–A1522. [doi:10.1137/16M1106122](https://doi.org/10.1137/16M1106122).